Long-Range Effects in Ion-Implanted Metallic Materials

Yu.P. Sharkeev, E.V. Kozlov*

ISPMS, Siberian Branch of Russian Academy of Sciences, 2/1 Academicheskii pr., Tomsk, 634021, Russia, phone:+7 3822 286911, fax: +7 3822 259576, E.mail: sharkeev@ispms.tsc.ru
** TSUAB, 2 Solyanay sq., Tomsk, 634021, Russia*

Abstract – The review and the analysis of the scientific literature data published by authors of the paper and the other authors on manifestation of the long-range effects in metals and alloys at ion implantation are presented. The description of the long-range effects observed in metals and alloys at ion implantation is given on the basis of experimental data. The analysis of regularities and mechanisms of the long-range effects is executed, its physical nature is considered.

1. Introduction

Investigating the physical processes taking place at interaction of the accelerated ions with solids the main attention is concentrated on the thin surface layer of the target, the thickness of which corresponds approximately to the ion projected range. At mean ion energy (10–10^3 keV) the depth of the ion penetration is not more than several tens or hundreds nanometers. A change of a chemical compound (alloying) and structures is occurred in this thin surface layer at ion implantation. In the surface layer the formation of precipitates and metastable phases is noticed, the crystal lattice transformation is carried out, amorphization is occurred, the irradiated defects are generated, the dislocation structure of high density is formed, etc. Results of experimental and theoretical research of the processes taking place in the surface ion-alloyed layer at bombardment of targets by accelerated ions, are submitted in numerous articles, tens monographs and reviews. Now it is possible to consider that the nature of the processes occurring in the target surface layer alloying at ion implantation has been well investigated. The theoretical models and experimental data allow to predict and to forecast those changes, which occur in the target surface layer at ion implantation.

Meanwhile, many experimental facts obtained at investigation of various properties and microstructures of the ion implanted materials testify that influence of ion fluxes at an irradiation of some semi-conductors, metals and alloys is not limited by the thin surface layer where the introduced ions are stopped but expanded to essentially large distances. Such results have been obtained, while investigating such mechanical properties as microhardness, wear resistance, friction coefficient, etc. The phenomenon of changing the microstructure and properties at the distances considerably exceeding the thickness of the surface layer alloyed at ion implantation has been termed as the long-range effect.

2. The Basic Results

The most important experimental data are systematized from the scientific periodic literature about the long-range effects in the solids subjected to ion – beam treatment (Table 1). The initials and surnames of the authors who were carrying out the investigations, a time interval during which authors published the data, a material of the target exposed to ion implantation, parameters of ion implantation, the investigation methods and the basic results can be found in the table. All data are presented in the chronological order of their publication. The table covers the period from 1973 up to 2004. Because of a format of the paper the list of primary articles are not presented in the table. Full information about the list of publications can be found in [1–8].

Table 1. Experimental data of the long-range effects at ion implantation

№ п/п	Authors, years of publications	Target materials	Parameters of ion implantation (sort of ions, ion energy, ion doze, etc.)	Methods of research observations
1	P.V. Pavlov, D.I. Tetelbaum, etc., 1973–2003	Si monocrystals, permalloy, foil thickness is 20–25 μm	B, N, P, Ar, 40 keV, ion current is 3–8 μA,· $1\cdot10^{13}$–$1\cdot10^{16}$ ion·cm^2	Change of microhardness on a surface that is opposite to irradiated surface
2	V.N. Chernikov, A.P. Zaharov, 1978–1989	Mo monocrystals	H, He, glow discharging, an accelerating voltage is 400–500 keV	Transmission electron microscopy. Change of dislocation structure on the depths exceeding the ion projected range in thousands times; high density of screw dislocations were observed on distance of 20 μm from the irradiated surface

№ п/п	Authors, years of publications	Target materials	Parameters of ion implantation (sort of ions, ion energy, ion doze, etc.)	Methods of research observations
3	M.I. Guseva, 1982	Stainless steel	Ni, 50 keV; H, 40 keV, $1 \cdot 10^{18}$ ion·cm^2	Increase of microhardness in the subsurface layer the thickness of which was up to 200 μm
4	V.M. Anishik, V.V. Yglov, etc., 1983, 1984	Ni and B polycrystals	B, C, 40…60 keV, $5 \cdot 10^{15}$…$4 \cdot 10^{17}$ ion·cm^2	X-ray method with use of a sliding beam, measurement of microhardness. Increasing microhardness in the subsurface layer up to depths of 5.0–6.0 μm, change of interplanar spacing takes place in subsurface layer on depth of 300 … 500 μm
5	Yu.A.Perlovich, etc., 1983–1984	W, Mo, Nb, Cu and B polycrystals	D, H, 25 keV, $5 \cdot 10^{17}$ ion·cm^2	X-ray analysis. Change of the of maxima form of polar figures; structural changes on depths in 10^4 times exceeding the ion projected range in metal
6	A.N. Didenko, A.E. Ligachev, I.B. Kyurakin, 1987	Armko-iron, Cu, steel	N, C, B, Ti, Mg, Al, W, Re, Pb, TiC complexes, ZrC, TaC, 20–200 keV, $1 \cdot 10^{13}$ – $1 \cdot 10^{19}$ ion·cm^2	Measurement of microhardness on the inclined cross-sections. Increase of microhardness and wear resistance occurs in the subsurface layer thickness of which is equal to 100–120 μm
7	Yu.P. Sharkeev, E.V. Kozlov, A.N. Didenko, A.I. Ryabchikov, etc., 1987–2002	α-Fe, Cu, Mo, alloys: Cu–Co–Al and Ni_3Fe, ВТ18У	C, N, Fe, W, Hf, Ni, Dy, La, B, Ar, 30–150 keV, $1 \cdot 10^{16}$–$1 \cdot 10^{18}$ ion·cm^2	Transmission electron microscopy, X-ray analysis. Formation of dislocation structures in subsurface layer thickness of which is equal to 50 μm and more
8	A.A. Taran, Z.B. Baturecheva, E.F. Chaikovskii, 1988	W monocrystals	Ar, 15 keV, $1 \cdot 10^{19}$ – $1 \cdot 10^{20}$ ion·cm^2	Rearrangement of dislocation structures and increase of dislocation density in subsurface layer thickness of which is equal to 15 μm
9	E. Friedland, etc., 1988–1996	Monocrystals: Ni, Cu, Au, Ag, Pd, Fe, Mo, Co, Re	Ar, Kr, Xe, O, C, Ne, 130, 150 and 720 keV, $1 \cdot 10^{15}$, $5 \cdot 10^{15}$, $1 \cdot 10^{15}$ ion·cm^2	Method of α-particle channeling in geometry of back scattering. Width of experimental distribution of point defects is in several times more than width of concentration defect profiles calculated
10	V.V. Ovchinnikov, etc., 1989–2003	Alloys of systems: Fe–Ni, Fe–Ni, Fe–Al, Fe–Si; $FePd_2Au$ alloy	N, Ar, continuous and repetitively pulsed modes, 20–40 keV, $6 \cdot 10^{14}$–$1 \cdot 10^{18}$ ion·cm^2	Mossbauer effect method. Redistributions of atoms and structural – phased transformations of non-thermal nature on depths in 10^3–10^4 greater than the ion projected range
11	V.S. Khmelevskaya, V.G. Malinkin, etc., 1989– 2003	Ni polycrystals, Mo monocrystals and polycrystals, alloys of systems: Fe–Cr, Fr–Ni, Fe–Cr–Ni, Ni–Cr, Cu–Ni, V–Ti–Cr, stainless steels	Ar, 20 keV, 40 keV, 1 MeV, $5 \cdot 10^{16}$–$3 \cdot 10^{18}$ ion·cm^2, 20–600 °C	X-ray analysis, transmission electron microscopy and measurement of the Vikkers microhardness. Structural-phased transformations and increase of microhardness in subsurface layer thickness of which is equal to 6 μm
12	N. N. Sutkin, V. A. Ivchenko, etc., 1990, 1994, 2000–2004	Cu_3Au alloy in the ordered state	Ar, 20 keV, $5 \cdot 10^{16}$ ion·cm^2 two modes of ion implantations: continuous and repetitively pulsed	Field ion microscopy. Dislocation pile-ups, sessile dislocation configurations and other defects on depths up to 0.2–0.5 μm
13	A.P. Komissarov, N.A. Mahlin, V.A. Polyakov, 1991	Ti, stainless steel	N, 1–10 keV	Increase of microhardness in subsurface layer the thickness of which on two and more orders more than the ion projected range
14	E.V. Kozlov, I.V. Tereshko, etc. 1991–1994, 1998	Ni, Fe, Cu, Mo polycrystals and Ni_3Fe alloy, P6M5 steel, hard alloy T15K6	Treatment in glow discharging at pressure of $1 \cdot 10^{-4}$ Pa, accelerating voltage is 0.8–3.0 keV, the ion current density is 0.1 μA·cm^2	Transmission electron microscopy, measurement of microhardness. The low-energy irradiation resulted in increasing of microhardness both on the irradiated and opposite surface sides (the sample size is 1 cm), increase of dislocation density and change of dislocation structure type through sample

№ п/п	Authors, years of publications	Target materials	Parameters of ion implantation (sort of ions, ion energy, ion doze, etc.)	Methods of research observations
15	B. Rauschenbach, 1992	α-Fe	N, B, 50,100, 200 keV, $1\cdot10^{16}$–$1\cdot10^{18}$ ion·cm^{-2}	Transmission electron microscopy. Formation of dislocation structures in the subsurface layer the thickness of which is more than 0.3 μm
16	E.M. Diasalidze, etc., 1992	yttrium oxide	Xe, 140, 300 keV, $5\cdot10^{16}$ ion·cm^{-2}	X-ray analysis. Structural changes in the subsurface layer exceeding thickness of the implanted zone in tens times
17	I.G. Romanov, etc., 1993	steels: R6M5, Y-10, 6H4M2FC	N, B, 40 keV, $3\cdot10^{16}$–$2\cdot10^{17}$ ion·cm^2 (continuous beam); Mo, 40 keV, $6\cdot10^{17}$ ion·cm^2	Increase of microhardness in the subsurface layer the thickness of which is up to 20 μm
18	G.V. Lisovs, L.S. Gudkov, V.M. Chermov, 1994	Iodide zirconium	B, 70 keV, $1\cdot10^{17}$–$5\cdot10^{17}$ ion·cm^{-2}	Measurement of microhardness. Effect of surface hardening on the depths exceeding 7 μm
19	A.J. Perry, D. Geist, etc., 1994–1998	TiN CVD and PVD coatings	N, Al, Ni, Zr, Hf, Cr, Mo, W, Y, Ti+Ni, 35, 70 and 90 kV, $0{,}5\cdot10^{17}$, $1\cdot10^{17}$, $1{,}8\cdot10^{17}$, $2{,}7\cdot10^{17}$, $3{,}2\cdot10^{17}$ ion·cm^{-2}	Method of diffraction of the parallel sliding x-ray beam. Ion implantation results in changing of residual stresses and microdeformation value in underlying layers
20	Guoyi Tang, etc., 1996	Zirconium alloy Zircaloy-4	N, 120 кэВ, $1\cdot10^{17}$–$1\cdot10^{18}$ ion·cm^{-2}, 100–724 °C	Transmission electron microscopy. Dislocation cells and high dislocation density are observed in subsurface layer that located beneath the ion implanted layer
21	I.G.Kozir', I.A.Tciganov, I.M.Charshakov, 1996	Armko-Fe	N, 10, 150 and 300 keV, $5\cdot10^{17}$ ion·cm^{-2}, sample temperature was not more than 100 °C	Thickness of the modified layer reaches 50 μm (the nitrogen ion projected range is ~250 nm); strong distortions of crystal structure and increase of its deficiency in part of grains depending on the grain crystal orientations are observed
22	Yu.P. Sharkeev, A.J. Perry, S.V. Fortuna, etc., 1998–2002	TiN CVD and PVD coatings	Ni+Ti, 70 кВ, total doze is $1\cdot10^{17}$ ion·cm^{-2}	Transmission electron microscopy. CVD coatings. Subgrains were formed in mother grains that are located beneath the implanted zone. PVD coatings. Relaxation of local internal stresses took place beneath the implanted zone
23	L.L.Meisner, A.I.Lotkov, V.P.Sivoha, etc., 1999–2003	Alloys on base of TiNi with shape memory form	Cu, Ti, Zr, Mo, $(0.1–5)\cdot10^{17}$ ion·cm^{-2}, 60 kV, 373–423 K	X-ray analysis, optical and scanner electronic microscopy, Auger electron spectroscopy, mechanical tests according to schemes of torsion and tension, measurement of microhardness. Change of a microstructural state and elastic and plastic behaviour under loading of subsurface layer the thickness of which is equal to 100 μm was observed
24	M.I. Guseva, Yu.V. Martinenko, A.M. Smislov, 2000	Ti–Al–Mo–Zr–Nb titanium alloy	N, C, B, Ar, $2\cdot10^{17}$ ion·cm^{-2}, 40 kV	Transmission and scanning electron microscopy, Auger electron spectroscopy. Considerable growth of microhardness and formation dislocation substructures of high density in subsurface layer with thickness of up to 50 μm were found
25	A.N. Tumetsev, A.D. Korotaev, etc., 2002	Mo polycrystals	Ti, Y, $1\cdot10^{17}$ ion·cm^{-2}, 50 kV	Transmission electron microscopy. Thickness of subsurface layer with defect substructure reached 30 μm; formation of a substructure with low angle disorientations took place in the layer of 10 μm thickness, cell nondisoriented substructures were formed in a layer thickness up to 20 μm and substructures with chaotic distribution of dislocations in a layer thickness up to 30 μm were revealed

The analysis of the data published shows that a number of researchers during long time were engaged in experimental studying of the long-range effects. Among them P.V. Pavlov, D.I. Tetelbaum (Nizhnii Novgorod), V.V. Ovchinnikov, N.N. Syutkin (Ekaterinburg), V.S. Hmelevskaya, V.G. Malynkin (Obninsk), E. Friedlend (South Africa), Antony J. Perry (Switzerland) and D. Geist (England), I.V. Tereshko (Belorussia), M.I. Guseva (Moscow). A.I. Ryabchikov (Tomsk), A.N. Didenko (Moscow) and authors of the paper who made a great contribution to the investigation of the long-range effects. Seemingly, P.V. Pavlov and D.I. Tetelbaum have made the first reference about the long-range effect in 1973. They reported on the change of the lattice parameter and the lifetime of non-basic charge carriers up to depths of several tens micrometers at ion irradiation of silicon.

All experimental results presented in the table can be divided into two groups. It is necessary to include in the first group the articles where authors have registered essential changes of physical and mechanical characteristics (microhardness, wear resistance) for various materials on depths from several up to tens (and even hundreds) micrometers.

It is necessary to note that measurement of microhardness is one of widespread methods for estimation of mechanical characteristics. At measuring of the microhardness of materials subjected to ion implantation, there is a set of problems of methodical character. Firstly, at any standard loading on indenter the depth of its penetration considerably exceeds the ion implanted layer thickness. Therefore microhardness of two layers are measured. They are the implanted layer and the underlaying layer that is not alloyed but where the defect structure is formed. In this case it is practically impossible to share the contribution to microhardness from these two layers. This problem can be solved partly at measuring microhardness on the inclined cross-sections or at supersmall loadings using the nanoindention method. It is necessary to note, that the data of the microhardness and wear resistance measurement in the ion-implanted materials are not the direct proof of the long-range effects.

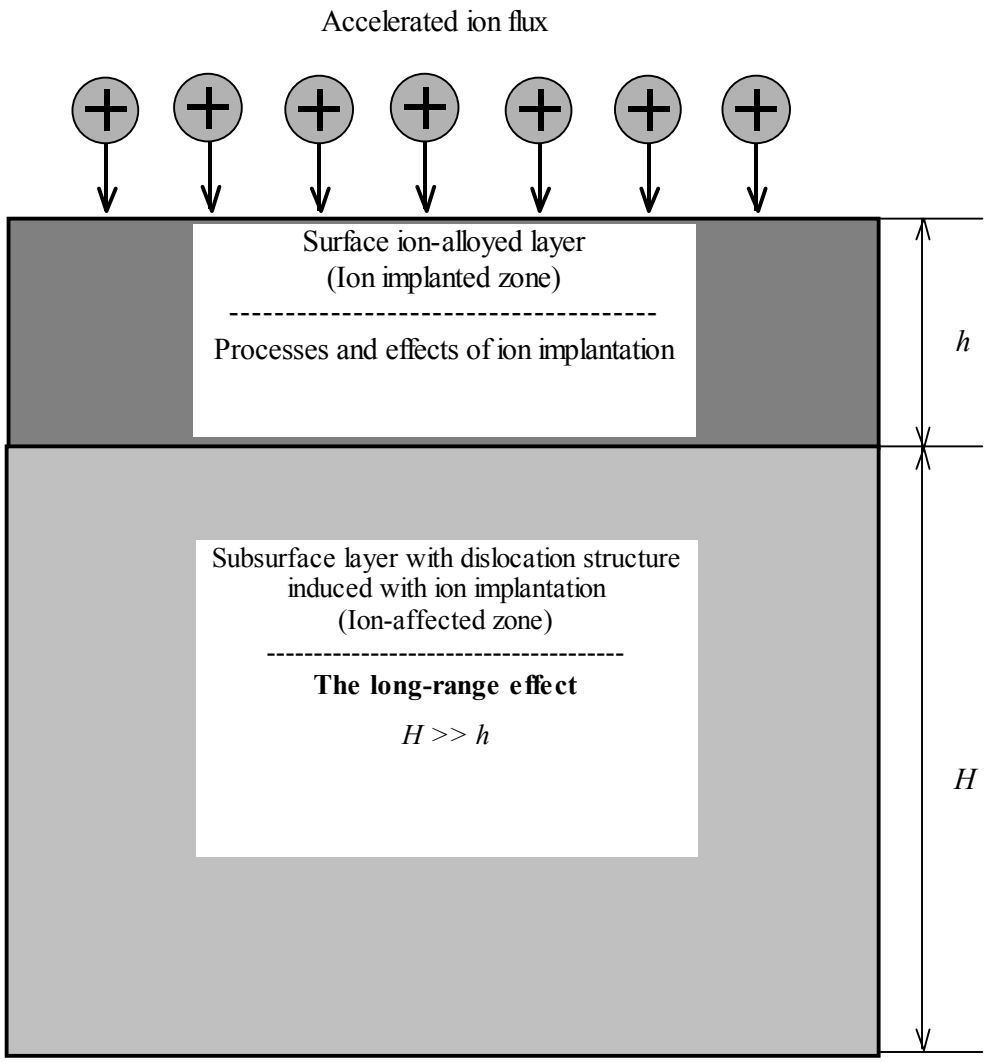

The long-range effect in metal materials at ion implantation

The second group of articles reveals: a) an abnormal deep deposition of the defects (dislocation loops, pores, point defects and point defect clusters) induced with ion irradiation; b) a formation of dislocation structures and change of structural-phased state in the subsurface layers the thickness of which is much greater than the thickness of the surface layer alloyed at ion implantation. As research methods the authors used various methods: a method of α-particle channeling, transmission electron microscopy, X-ray analysis, field ion microscopy, a Mossbauer effect method and other methods. Obviously, the experimental results presented in the articles of the second group are the direct proof of the long-range effect manifestation at ion implantation of crystals.

3. Conclusion

As a result of the analysis of literature data and our own data the following conclusions about the long-range effect in ion-implanted metals and alloys are offered.

The long-range effects in metals and alloys consist of the change of a defect structure and/or a structural – phased state in the subsurface layer (the ion-affected zone) of the ion implanted target, directly located beneath the surface layer (the implanted zone) in which the implanted ions are stopped (see figure). Thickness of the ion-affected zone with the microstructure modified at ion implantation varies from several up to tens micrometers and more. In annealed metals with low density of dislocations the long-range effects are manifested, first of all, in the dislocation generation, the increase of dislocation density at 1–1.5 orders of magnitude and the formation of dislocation substructures.

At the same time, with the formation of dislocation structure a subsystem of dislocation loops is formed in the ion-affected zone of metal target at ion implantation. Dislocation loops in the ion-affected zone are generated by condensation of point defects, which diffused from the implanted zone, and also point defects generated by dynamic of screw dislocations from the implanted zone into the ion-affected zone. The dislocation loops can be formed in the implanted zone and subsequently move from the implanted zone into ion-affected zone as a result of the elastic interaction between dislocation loops.

The dislocation substructures, which form in the ion-affected zone of the metal target during ion implantation, are similar to the dislocation substructures generated in metals deformed from several to 10–15%. The dislocation substructures formed in the ion-affected zone after ion implantation are non-disoriented. Six types of non-disoriented dislocation substructures were observed. They were cell dislocation substructure, cell-net dislocation substructure, dislocation tangles, net dislocation substructures, dislocation pile-ups, and the substructure with the chaotic dislocation distribution. The dislocation substructure formation corresponds with the processes of self-organizing of dislocation structure generated during ion implantation in the metallic target.

The dislocation scalar density in the ion-affected zone of the target with distance from the irradiated surface varies in the non-monotonic way. Typical dependence of the scalar dislocation density on distance up to the irradiated surface subjected is a curve with the maximum localized at 10–15 μm from the surface. A maximum of the dislocation density in the ion-affected zone increases linearly with increasing in radius and mass of the implanted ions. The thickness of the ion-affected zone with changed dislocation structure and magnitude of the dislocation density in the ion-affected zone increase with the ion doze. The dislocation density is also raised when the ion doze rate is increased.

The formation of dislocation structures in the ion-affected zone takes place not only in well-annealed metals with a low dislocation density and also in the metals deformed not more than 10–15%. The substructural hardening reduces the value effect up to its full disappearance. Heavily deformed metals do not exhibit the long-range effect where a high dislocation is already presented. There is a limit of substructural hardening at which the long-range effect is suppressed.

The type of strengthening (solid solution, grain boundary, dispersed, multi-phased) and the value of strengthening play an important role in the development of the long-range effects. The presence of barriers for dislocation motion (high dislocation density, grain boundaries, second phase interlayers, dispersed particles, etc.) reduces the long-range effects. The major requirements of the development of the long-range effects are low yield strength and a low dislocation density in the initial state of the target.

In the ion-affected zone, mechanical and other properties can be changed noticeably. Changes in these properties can take place in the subsurface layers. The thickness of the modified subsurface layers varies from several up to tens of micrometers

The ion implantation is accompanied by the formation of considerable mechanical stresses, which have a static and/or dynamic character. Experimental data and theoretical estimations show that the stresses generated at a high ion dose can reach a value of 10^3 MPa. Such high stress exceeds the yield strength of the implanted materials. These stresses are sufficient for initiating mechanisms of dislocation accumulation in the ion-affected zone of the target.

In the ion-affected zone the dislocations are generated by injection of dislocations, dislocation loops and point defects from the implanted zone and by plastic deformation of the ion-affected zone.

The mathematical model of a dynamic motion of dislocations proposed allows to explain the long-rang effects in ion-implanted metallic materials. Under the

influence of stresses generated in the target, the dislocations moving within the implanted zone reach high velocities and high kinetic energies. This leads to their ejection into the ion-affected zone where the dislocations moving by inertia traverse distances greater than the thickness of the implanted zone, comparable with the ion-affected zone thickness. During ion implantation, dislocation accumulation takes place in the ion-affected zone.

References

[1] Yu.V. Martynenko, *Itogi nauki i tehniki Puchki zaryajennih chastits I tverdoe telo.* Moscow, VINITI, 1993, V. **7,** pp. 82–112.

[2] Yu.P. Sharkeev, A.N. Didenko, E.V. Kozlov, Izvestiya vuzov. Fizika, No. 5, 92 (1994).

[3] Yu.P. Sharkeev, A.N. Didenko, E.V. Kozlov, Surf. Coat. Techn. **65**, 112 (1194).

[4] A.L. Pivovarov, Metallofizika i noveishie technologii **16**, No. 12, 3 (1994).

[5] Yu.R. Kolobov, Yu.P Sharkeev, V.G. Abdrashitov, O.A. Kashin, *in: Physical Mesomechanicsof Heterogeneous Media and Computer-Aided Design of Materials* (Edited by Victor E. Panin), Cambridge International Science Publishing, 1998, Chapter 15, pp. 312–336.

[6] Yu.P. Sharkeev, E.V. Kozlov, A.N. Didenko, Surf. Coat. Techn. **96/1**, 103 (1997).

[7] Yu.P. Sharkeev, E.V. Kozlov, Surf. Coat. Techn. **158–159**, 219 (2002).

[8] Yu.P. Sharkeev, S.N. Kolupaeva, N.V. Girsova, N.V. Vihor, S.V. Fortuna, L.E. Popov, E.V. Kozlov, Metalli, No. 1, 109 (1998).